Supplementary Information

Influence of conversion time and precursor density on the orientation of vapor-deposited ZIF-8

Marianne Kräuter[1]*, Alexander John Cruz[2], Timothée Stassin[2], Sabina Rodríguez-Hermida[2], Rob Ameloot[2], Roland Resel[1], Anna Maria Coclite[1]

[1] Institute of Solid State Physics, Graz University of Technology, Petersgasse 16, 8010 Graz, Austria
[2] Center for Membrane separations, Adsorption, Catalysis, and Spectroscopy (cMACS), KU Leuven, Celestijnenlaan 200F, 3001 Leuven, Belgium
*marianne.kraeuter@tugraz.at; +43 316 873 - 8467

Table S1. Overview of the varied deposition parameters and of the properties of the synthesized ZIF-8, which were investigated to discern the impact of the varied deposition parameters.

Varied parameters	Investigated properties of ZIF-8
precursor (ZnO) thickness	crystallinity and crystallographic orientation
precursor (ZnO) density	morphology and spread on substrate
conversion time	lateral and vertical crystallite size
	layer roughness
	layer thickness

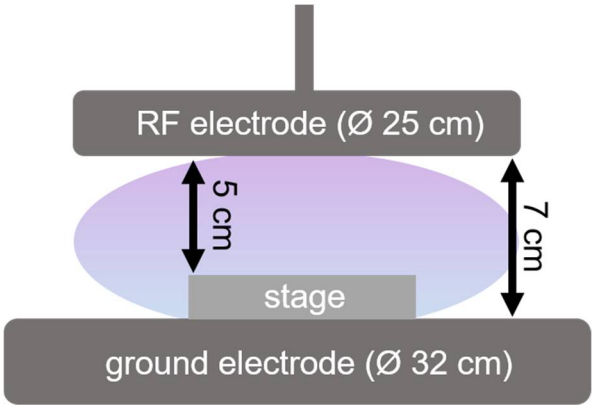

Figure S1. Schematic of the custom direct plasma atomic layer deposition reactor. The stage can be removed from the chamber, changing the distance between the electrodes from 5 cm to 7 cm.

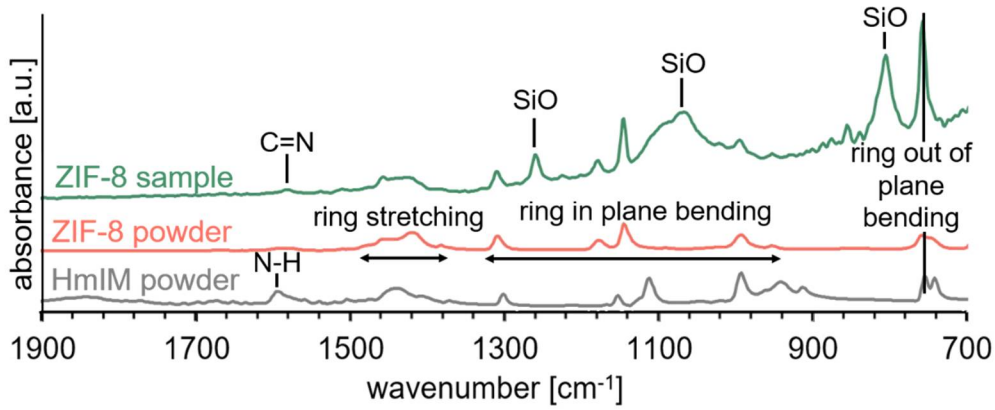

Figure S2. ZIF-8 obtained from a ZnO layer with a density of ϱ = (4.6 ± 0.1) g/cm³ deposited for 60 cycles measured via attenuated total reflection Fourier-transform infrared spectroscopy. Reference data of ZIF-8 powder and 2-methylimidazole-powder are shown for comparison.

Figure S2 serves to show that the obtained layer matches the chemical fingerprint of ZIF-8. The N-H stretch is not visible in the ZIF-8 spectra but can be seen in the HmIm powder spectrum at 1590 cm^{-1}. Between 1600 cm^{-1} and 1000 cm^{-1} the C-C, C=C, and C=N bonds of ZIF-8 become visible: From around 1480 cm^{-1} to 1380 cm^{-1} the stretching of the entire ring of ZIF-8 can be observed. Between 1305 cm^{-1} and 950 cm^{-1} the ring in-plane bending becomes visible, the peak at 755 cm^{-1} indicates the ring out-of-plane bending. The peaks at 1260 cm^{-1}, 1065 cm^{-1}, and 805 cm^{-1} are Si-O peaks arising from the native oxide of the substrate.

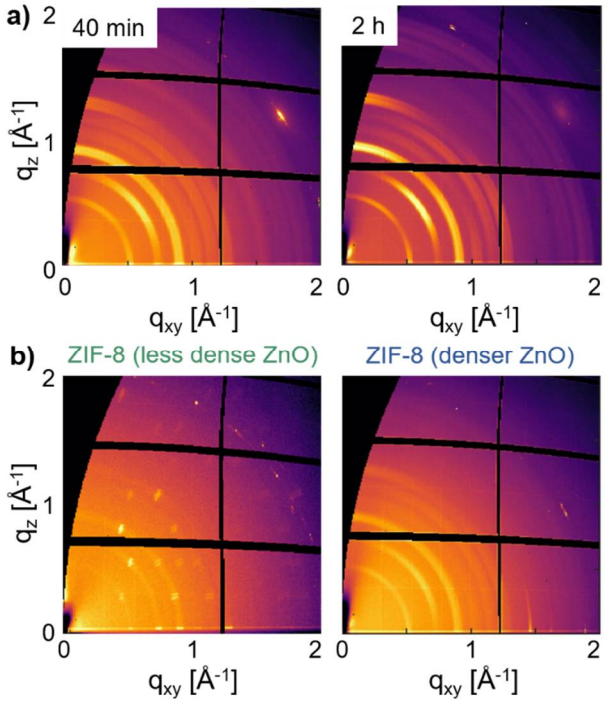

Figure S3. Grazing incidence X-ray diffraction data of ZIF-8 (a) grown from denser ZnO deposited for 60 cycles with conversion times of 40 min and 2 h. (b) obtained from ZnO deposited for 6 cycles with densities of ϱ = (4.6 ± 0.1) g/cm³ and ϱ = (5.2 ± 0.2) g/cm³ after 24 h of conversion.

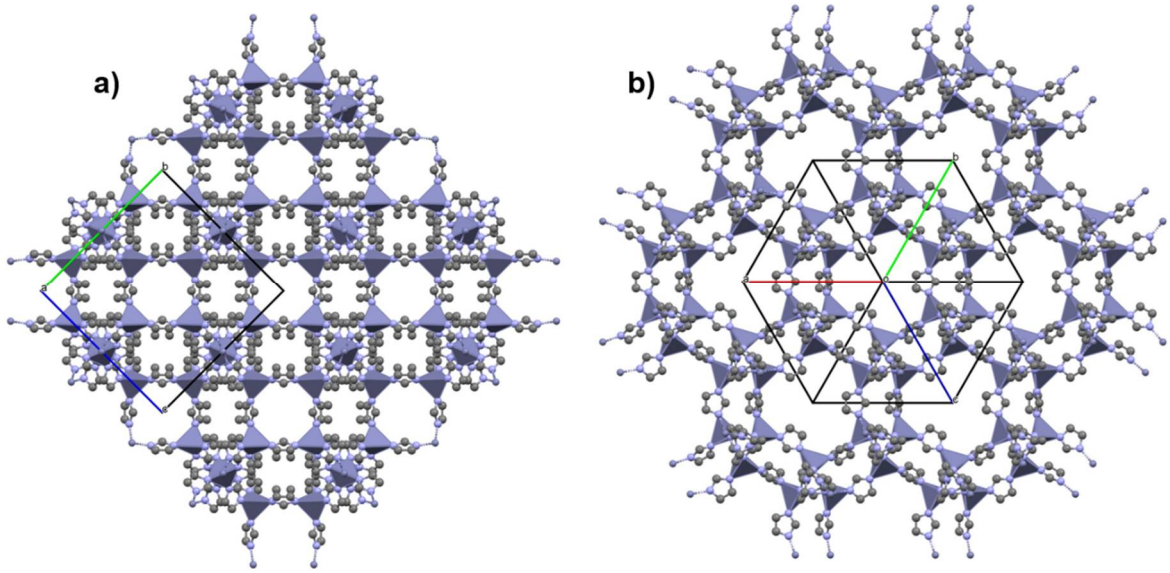

Figure S4. Structure of ZIF-8 plotted in Mercury. Dark-blue polyhedra correspond to zinc, pale-blue spheres to nitrogen and grey spheres to carbon. Hydrogen is not depicted for sake of clarity. The images show the top-down view of the (a) (100) and (b) (111) plane.

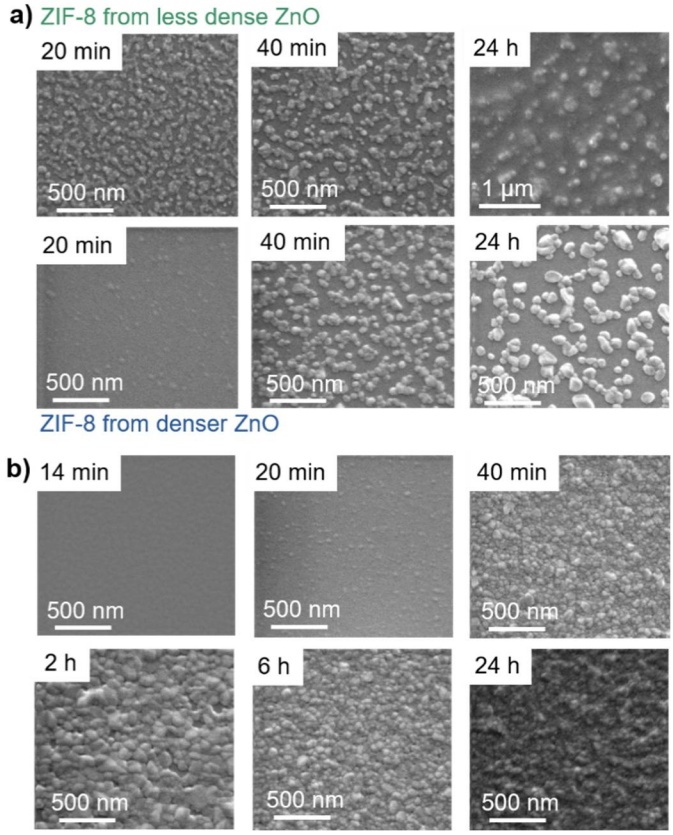

Figure S5. Scanning electron microscopy data showing ZIF-8 (a) obtained from ZnO layers deposited for 6 cycles with densities of $\varrho = (4.6 \pm 0.1)$ g/cm^3 and $\varrho = (5.2 \pm 0.2)$ g/cm^3 after different conversion times. (b) grown from denser ZnO deposited for 17 cycles after different conversion times.

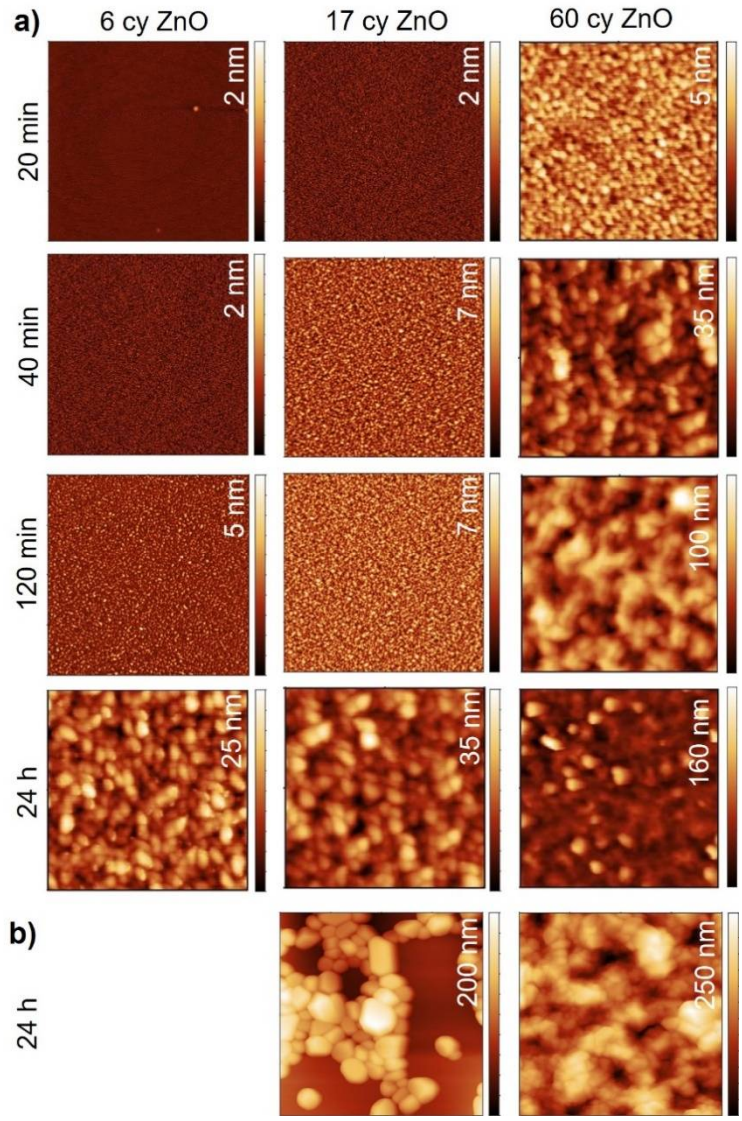

Figure S6. Atomic force microscopy topography images showing ZIF-8 (a) obtained from ZnO layers deposited for 6, 17 and 60 cycles with a density ϱ = (5.2 ± 0.2) g/cm^3 after different conversion times. (b) grown from ZnO with a density of ϱ = (4.6 ± 0.1) g/cm^3 deposited for 17 and 60 cycles after 24 h. All images are 2x2 μm in size; the color scale of each image was individually adjusted for sake of visibility.